## FosGFP expression does not capture a sensory learning-related engram in superficial layers of mouse barrel cortex

Jiseok Lee<sup>a</sup>, Joanna Urban-Ciecko<sup>b</sup>, Eunsol Park<sup>a</sup>, Mo Zhu<sup>a</sup>, Stephanie E. Myal<sup>c</sup>, David J. Margolis<sup>d</sup>, and Alison L. Barth<sup>a,1</sup>

<sup>a</sup>Department of Biological Sciences, Carnegie Mellon University, Pittsburgh, PA 15213; <sup>b</sup>Nencki Institute of Experimental Biology of the Polish Academy of Sciences, 02-093 Warsaw, Poland; <sup>c</sup>University of Pittsburgh School of Medicine, Pittsburgh, PA 15213; and <sup>d</sup>Department of Cell Biology and Neuroscience, Rutgers, The State University of New Jersey, Piscataway, NJ 08854

Edited by Liqun Luo, Department of Biology, Stanford University, Stanford, CA; received July 13, 2021; accepted November 7, 2021

Immediate-early gene (IEG) expression has been used to identify small neural ensembles linked to a particular experience, based on the principle that a selective subset of activated neurons will encode specific memories or behavioral responses. The majority of these studies have focused on "engrams" in higher-order brain areas where more abstract or convergent sensory information is represented, such as the hippocampus, prefrontal cortex, or amygdala. In primary sensory cortex, IEG expression can label neurons that are responsive to specific sensory stimuli, but experiencedependent shaping of neural ensembles marked by IEG expression has not been demonstrated. Here, we use a fosGFP transgenic mouse to longitudinally monitor in vivo expression of the activitydependent gene c-fos in superficial layers (L2/3) of primary somatosensory cortex (S1) during a whisker-dependent learning task. We find that sensory association training does not detectably alter fosGFP expression in L2/3 neurons. Although training broadly enhances thalamocortical synaptic strength in pyramidal neurons, we find that synapses onto fosGFP+ neurons are not selectively increased by training; rather, synaptic strengthening is concentrated in fosGFP- neurons. Taken together, these data indicate that expression of the IEG reporter fosGFP does not facilitate identification of a learning-specific engram in L2/3 in barrel cortex during whisker-dependent sensory association learning.

c-fos | engram | learning | plasticity | barrel cortex

he coupling of immediate-early gene (IEG) transcription with fluorescence markers has been used to identify and monitor neurons that are part of a select ensemble engaged during learning. Elevated activity in a subset of neurons is widely assumed to promote the recruitment of these neurons into a memory engram that can drive selective recall. IEG expression has been used to identify neurons that are part of a memory engram in the hippocampus, prefrontal cortex, and amygdala among many brain regions, where the increased and stimulus-specific activation of individual neurons is thought to promote their capture of selective synaptic change during learning (1). Recent studies indicate that IEG-guided selective reactivation of a small neural ensemble can drive a learned behavioral response even in the absence of the stimulus, providing critical support for the engram hypothesis (1). However, these experiments were carried out in brain areas where individual neurons have highly abstract response properties that can remap according to complex inputs defined by multimodal cues. It remains unknown whether IEG expression in primary sensory cortex is associated with the recruitment of specific neurons into a "memory" engram, although experience-dependent changes in synaptic strength and population response properties have been well characterized.

At least a subset of neurons in sensory cortex are tuned to specific sensory features, such as frequency in the auditory system (2) or line orientation in the visual system (3). When animals are trained to associate a specific sensory input with a rewarded outcome or a punishment, stimulus-specific neural activity, even in primary sensory cortex, can be enhanced (4–7). In addition, there is abundant evidence for experience-dependent plasticity in sensory neocortex, both in synaptic changes (8–12) as well as increased stimulus-evoked firing (4–7, 13–15). Thus, primary sensory cortex is an excellent place to evaluate how IEG expression can reveal an engram that develops during the course of sensory learning and is linked to plasticity at the cellular level.

We hypothesized that sensory association training (SAT) would stabilize or expand an ensemble of neocortical neurons marked by IEG expression under basal conditions. We examined this prediction in the mouse barrel cortex, where previous studies have shown that neurons expressing a fosGFP transgene show elevated spontaneous and evoked firing (16–19) and are tuned to multiwhisker stimulation, in part due to stronger input from the posterior-medial (POm) nucleus of the thalamus (18). In an attempt to consolidate this ensemble during learning, we used a SAT task in which a multiwhisker stimulus was paired with a water reward. Recent work from our laboratory has shown that POm thalamocortical synapses onto L2/3 pyramidal neurons in wild-type mice undergo synaptic potentiation during

## Significance

Activity-dependent, immediate-early gene (IEG) expression has been used to label and reactivate specific subsets of neurons involved in memory encoding in the hippocampus, amygdala, and prefrontal cortex. Although neurons in primary sensory cortex are changed by learning, previous studies have not linked IEG expression to a learning-related engram in this brain area. We longitudinally monitored expression of a fosGFP transgene in mouse barrel cortex during a whisker-dependent sensory association learning. Surprisingly, we found that sensory training does not alter fosGFP expression in L2/3 neurons and that thalamocortical synaptic potentiation is not concentrated in fosGFP-expressing neurons. These data show that a learning-related neural ensemble in primary sensory cortex is not revealed by expression of a transgenic reporter of the IEG c-fos.

Author contributions: J.L., D.J.M., and A.L.B. designed research; J.L., J.U.-C., E.P., M.Z., and S.E.M. performed research; J.L., J.U.-C., E.P., M.Z., and S.E.M. analyzed data; and J.L., D.J.M., and A.L.B. wrote the paper.

Competing interest statement: A.L.B. has a patent on the fosGFP transgenic mice.

This article is a PNAS Direct Submission.

Published under the PNAS license.

This article contains supporting information online at http://www.pnas.org/lookup/suppl/doi:10.1073/pnas.2112212118/-/DCSupplemental.

Published December 20, 2021.

<sup>&</sup>lt;sup>1</sup>To whom correspondence may be addressed. Email: barth@cmu.edu.

this SAT paradigm (12). Since spike-timing—dependent plasticity rules predict that presynaptic inputs followed by postsynaptic spiking are more likely to undergo long-term potentiation (20) and fosGFP+ neurons are more likely to fire with multiwhisker stimulation or POm activity (18), we predicted that thalamocortical synaptic plasticity after SAT would be concentrated in this more-active ensemble.

Our experiments were twofold. First, we directly imaged fosGFP expression across multiple days of SAT to determine whether this behavioral manipulation might enhance or stabilize labeled neurons, before and after learning. Second, we examined how POm thalamocortical synapses onto fosGFP+ neurons were altered during SAT. Our results indicate that enhanced fosGFP expression is not correlated with SAT or POm input plasticity. Instead, thalamocortical synaptic potentiation was concentrated in neighboring fosGFP— neurons. These data indicate that fosGFP expression in superficial layers of primary sensory cortex does not facilitate identification of a neuronal ensemble correlated with learning.

## Results

Sensory Association Learning in a Whisker-Dependent Task. To assess learning-related dynamics in fosGFP-labeled neuronal ensembles in superficial layers of mouse barrel cortex, we used a whisker-dependent sensory association task for training freely moving animals in their home cage where animals received a gentle air puff (500 ms, 6 psi) to the right facial vibrissae 500 ms before delivery of a water reward (21) (Fig. 1 A and B). FosGFP mice were implanted with a cranial window over S1 barrel cortex and recovered for several days before the onset of daily imaging (Fig. 1C). Control fosGFP animals were housed in the training cage where water was delivered from the lick port but without any coupled sensory stimulus (Fig. 1D). For the training group, mice were housed in the training cage 24 h prior to the pairing of a multiwhisker stimulus with a water reward to acclimate to the new environment. Although animals were adults (2 to 4 mo old) and underwent brief isoflurane anesthesia for daily imaging, all trained animals showed a significant difference in anticipatory licking in stimulus trials after 5 d of training (Fig. 1E), indicating that neither age nor repeated imaging prevented learning.

Monitoring fosGFP Expression During Acquisition of a Sensory Association Task. IEG expression has been used to identify neurons engaged during learning. Typically, this has been studied in the hippocampus (22-25), the amygdala (26), striatum (27), hypothalamus (28), and high-order cortical areas such as the retrosplenial cortex (29, 30), secondary motor cortex (31), and prefrontal cortex (32-35). Although neurons in primary sensory areas can exhibit stimulus-specific IEG expression (36-38), it is unclear whether IEGs might be useful to mark specific neurons that are part of a learning engram. To test this idea, we monitored fosGFP expression during SAT in L2/3 of the barrel cortex. L2/3 in the neocortex is the site of synaptic plasticity (12, 39) as well as increased sensory-evoked responses (4–7) during sensory experience and association learning. We thus expected that SAT would increase fosGFP expression in individual cells that were initially labeled and/or by inducing fosGFP in a new ensemble.

L2/3 neurons in S1 barrel cortex were imaged daily to monitor training-dependent changes in fosGFP expression. Since animals were trained with a multiwhisker stimulus, our analysis was not restricted to a specific barrel column. Consistent with prior studies (16, 40), fosGFP expression was distributed across the cortical column (Fig. 2A). Previous studies report c-fos expression in both excitatory and inhibitory neurons but not glial cells in the barrel cortex (41). In accordance with this, fosGFP expression was restricted to neurons, as immunohistochemical analysis revealed that all fosGFP+ cells expressed the neuronal marker NeuN (Fig. 2 B and C). FosGFP fluorescence could be detected in ~35% of neurons under our imaging conditions (Fig. 2C); we note that many cells showed extremely low levels of fluorescence. The overwhelming majority of fosGFP neurons in L2/3 were pyramidal cells, consistent with prior studies.

Although absolute levels of fosGFP could change across days, fosGFP-expressing cells with a sixfold range of fluorescence intensity could be reliably tracked (Fig. 3A). Although fosGFP has a half-life of about 6 h (40), most fosGFP neurons could be detected across days, suggesting that the conditions for fos expression were maintained over time.

A day-to-day comparison of fluorescence intensity levels for the population shows that there was a small shift to either increase or decrease in intensity across any given 24-h interval

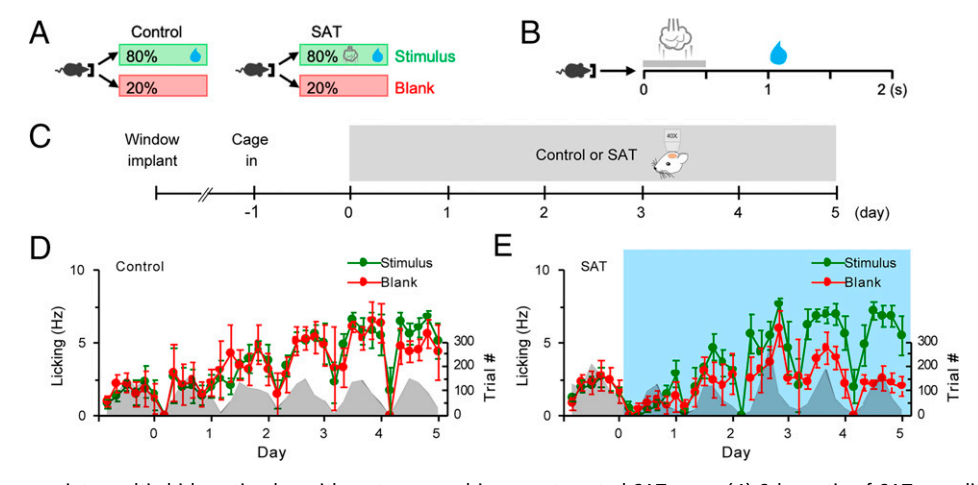


Fig. 1. Mice learn to associate multiwhisker stimulus with water reward in an automated SAT cage. (A) Schematic of SAT paradigm. In an automated training home cage, freely moving mice can initiate trials by nose poking a water port. In control, water is delivered with 80% probability per trial. In SAT, a gentle air puff is delivered followed by water delivery with 80% probability per trial. (B) Structure of a stimulus trial. Nose poke initiates delivery of an air puff followed by a small water drop 1 s later. (C) Schematic of longitudinal in vivo imaging. After recovery from cranial window surgery, mice were put into the training cage 1 d prior to imaging start. Imaging was done once every day for 5 d of control or SAT. (D) Anticipatory lick frequencies (mean  $\pm$  SEM) in stimulus and blank trials across 5 d of control. Trial numbers are shown in gray shade. n = 6 mice. (E) Same as in D for SAT. n = 7 mice. Blue shade, training window.

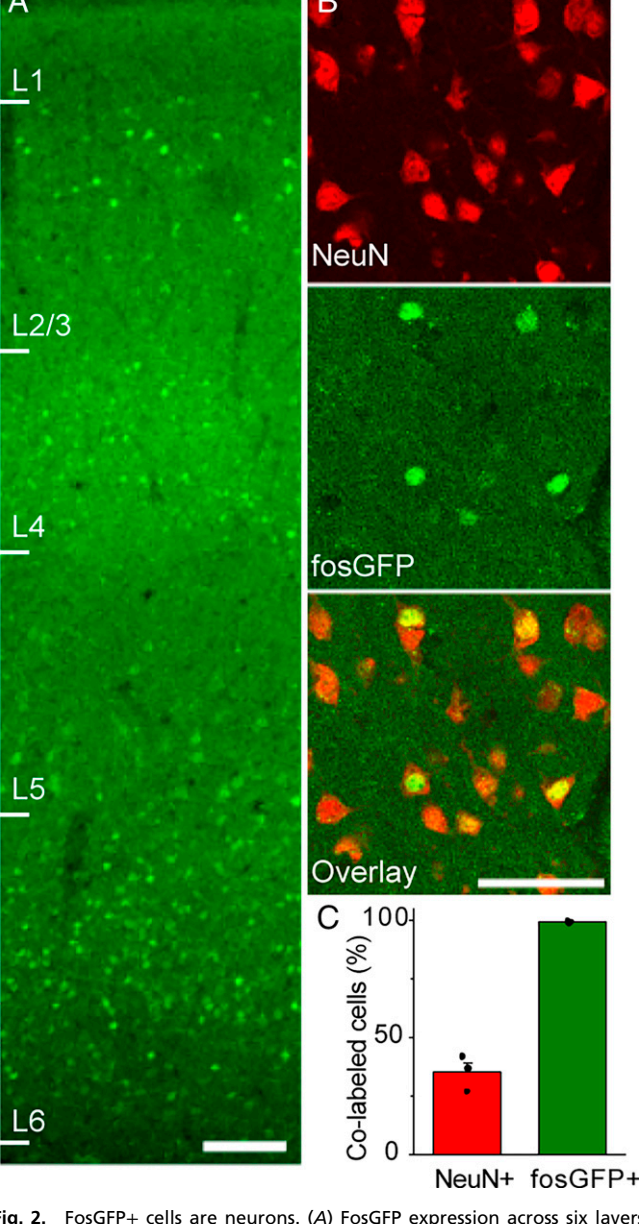


Fig. 2. FosGFP+ cells are neurons. (A) FosGFP expression across six layers in barrel cortex from a naïve mouse that was unexposed to training cage. (Scale bar, 100  $\mu$ m.) (B) Immunostaining of NeuN in barrel cortex L2/3 of brain sections from naïve fosGFP mice that were unexposed to training cage. (Scale bar, 50  $\mu$ m.) (C) Fraction (mean  $\pm$  SEM) of fosGFP+ cells out of NeuN+ cells and NeuN+ cells out of fosGFP+ cells. n=3 mice.

in control mice. For example, there was a small reduction in intensity from day 0 (at the onset of the imaging period) to day 1 in control animals (Fig. 3B), but from day 1 to day 2, there was a small increase and from day 2 to day 3 a small decrease (SI Appendix, Fig. S1). On average, these fluctuations were small and maintained throughout the imaging period and could not be attributed to changing environmental or behavioral cues.

Individual neurons could be aligned and tracked across days. To visualize small changes in fosGFP expression levels for detected neurons from control animals over time, we ranked cells according to fluorescence intensity from the first day (day 0) in the training cage and compared how intensity changed across subsequent days. The pool of analyzed cells was selected based upon fosGFP expression in any imaging day across the entire experiment; some cells might not show

expression on a given day. For individual neurons exhibiting fosGFP fluorescence, expression across time was dynamic. We observed that the brightest cells showed a strong tendency to decrease expression levels over both short and long time intervals; the majority (85  $\pm$  6%, n = 102 cells in six animals) of the top 20% brightest cells in each animal showed some reduction in their fluorescence signal over a 24-h window, on average by 0.7-fold (Fig. 3C). For longer time periods, this trend was similar (Fig. 3 D and E); after 5 d,  $87 \pm 4\%$  of the original group of these very bright cells reduced their expression. For fosGFP+ neurons with lower expression levels (bottom 20%), there was a trend toward increasing expression over longer (5-d) time intervals, where  $86 \pm 4\%$  of cells in this group (n = 102 cells) showed increased expression (1.2-fold). Overall, most detected neurons showed relatively stable levels of fosGFP expression over a 24-h time interval. We propose that fos expression in at least a subpopulation of L2/3 neurons may be maintained by some aspect of network function that slowly fluctuates over time.

FosGFP dynamics were remarkably similar for animals that underwent SAT. Surprisingly, we did not observe a marked increase in either the fluorescence intensity of labeled neurons or in the number of labeled neurons at the onset of training compared to control animals (Fig. 3F). There was no overall difference in the cumulative distribution of fluorescence signals with training, either at onset or after 5 d of training when all animals showed behavioral changes indicative of learning (Fig. 3G and I). These data indicate that sensory training does not drive increased fosGFP expression.

Tracking of individual neurons enabled a comparison of intensity changes across the SAT period. Ranking cells by fluorescence intensity on day 0 (the day prior to training onset) showed that the brightest cells tended to decrease fosGFP expression with the onset of SAT; on average, 79 ± 8% (n = 123 cells in seven animals) of the top 20% brightest cells reduced their expression over the first 24-h window (0.7-fold; Fig. 3H). This trend was enhanced over long time periods, where  $88 \pm 7\%$  of the original bright cells identified prior to training reduced their expression after 5 d of SAT (Fig. 3J). For fosGFP+ neurons with lower expression levels (bottom 20%), there was a modest trend toward increasing expression over longer time intervals during SAT, where  $93 \pm 4\%$  of cells in this group (n = 123 cells) showed increased expression (1.2-fold). These results were remarkably similar to what was observed in control mice housed in the training cage but without paired stimulus-reward coupling.

Overall, we find that SAT did not increase fosGFP expression. Slow fluctuations in fosGFP fluorescence suggests that expression may be maintained by some aspect of network function that slowly fluctuates over time, unrelated to training.

# FosGFP Expression in Individual Neurons Is Not Enhanced by SAT. Because longitudinal imaging allows us to track individual cells across days, we next examined whether SAT might influence the propensity for fosGFP fluorescence to either increase or decrease within a given cell. Our prior studies using wild-type animals showed that SAT strengthened POm inputs onto L2/3 neurons (12) and that fosGFP+ neurons receive larger inputs from POm compared to fosGFP- neurons (18). Thus, we predicted that stronger POm drive onto fosGFP neurons during SAT might further enhance levels of fosGFP in individual neurons.

To test this hypothesis, we compared fosGFP fluorescence intensity levels within a 24-h time period across the training period for both control and trained mice (Fig. 4). Changes in relative intensity for each cell were evaluated, since this method could detect small changes in cells irrespective of initial fluorescence signal. For example, a weakly labeled cell that increased fosGFP fluorescence might be indicative of the stabilization of

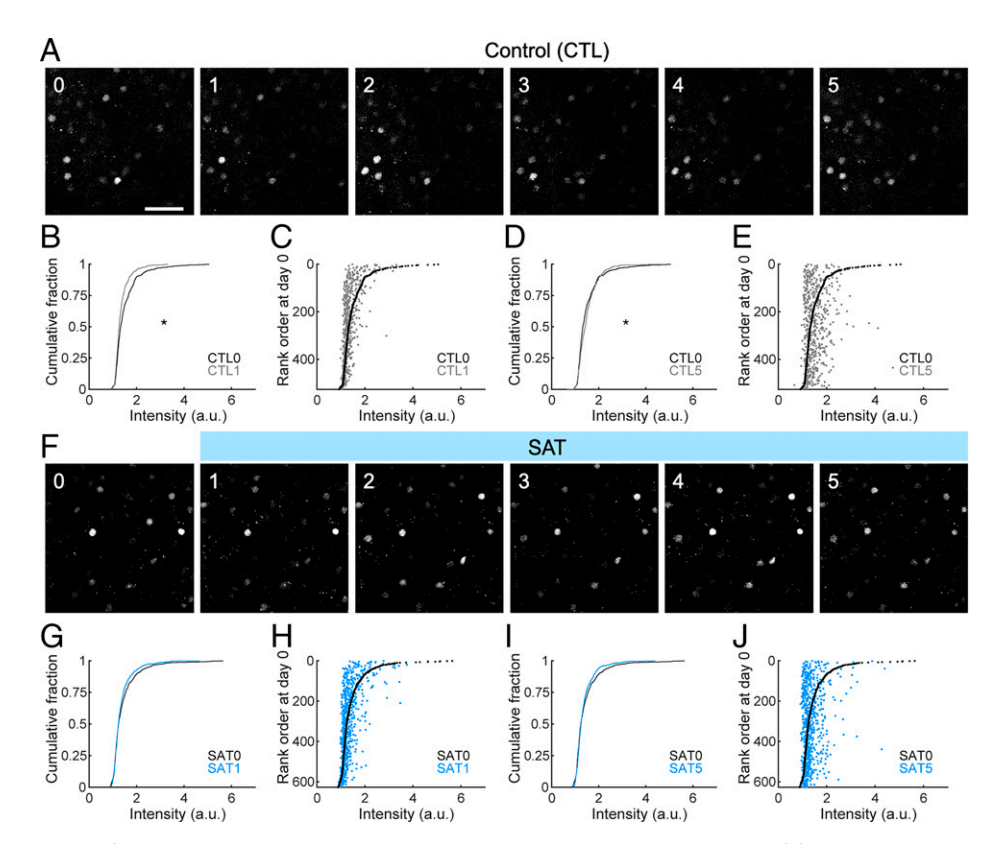


Fig. 3. SAT does not increase fosGFP expression relative to untrained control mice. (A) Example images of fosGFP-expressing cells in the barrel cortex L2/3 across 5 d of control (CTL). (Scale bar, 50  $\mu$ m.) (B) Comparison of the distribution of fosGFP intensities on day 0 and day 1 of control. Wilcoxon rank-sum test,  $P=1.5755 \times 10^{-6}$ . n=526 cells from six mice. a.u., arbitrary unit. (C) Cells were ranked according to fosGFP intensity on day 0. FosGFP intensity of each cell on day 0 (black) and day 1 (gray) of control was plotted against the rank order on day 0. (D) Comparison of the distribution of fosGFP intensities on day 0 and day 5 of control. Wilcoxon rank-sum test, P=0.0287. (E) Cells were ranked according to fosGFP intensity on day 0. FosGFP intensity of each cell on day 0 (black) and day 5 (gray) of control was plotted against the rank order on day 0. (F) Same as in A for SAT. (G) Same as in B for SAT. Wilcoxon rank-sum test, P=0.3065. n=627 cells from seven mice. (H) Same as in C for SAT. (I) Same as in D for SAT. Wilcoxon rank-sum test, P=0.8493. (J) Same as in E for SAT. P<0.05.

a new ensemble, although that small increase might not shift the average intensity of the population. Indeed, the mean fluorescence intensity of the imaged population was not significantly altered in trained animals compared to control throughout the imaging period (Fig. 44).

Cells were subdivided according to changes in relative intensity, based on whether their absolute intensity increased ("up") or decreased ("down") by more than 20% from the preceding day, a criterion that corresponded roughly to 1 SD from the mean intensity (Fig. 4 B and C). Cells that did not meet this criterion were classified as "stable." On average,  $\sim 80\%$  of cells did not change fluorescence intensity by more than 20% in either direction across a given 24-h window, although this value varied considerably across imaged animals in both control and trained mice (range:  $\sim 50$  to 100% of cells fell into the "stable" category for a given animal; Fig. 4E). The proportions of down, stable, and up cells were not obviously different between control and sensory association—trained mice at any period during training, and no comparisons for any category or time period were significantly different (Fig. 4D-G).

FosGFP Fluorescence Dynamics at the Time of Learning. The amount of training required for an animal to demonstrate increased anticipatory licking to the air puff stimulus could vary widely (range: 1 to 5 d of training), consistent with prior studies that have observed similar heterogeneity in learning trajectories across individual animals (21, 42). In this case, the animal-averaged data presented in Fig. 4 might obscure a more marked transition in fosGFP expression that occurred directly

around the learning interval within an animal. The day of learning was defined by comparing the lick frequency on stimulus and blank trials for the last 20% of trials on a given day (performance = lick\_water - lick\_blank) to determine when this difference became significant. This value abruptly changed during the training period (Fig. 5 A and B), suggesting that there may be discrete transitions in behavior across days.

We examined dynamics in fosGFP fluorescence for individual neurons for the 24-h window during which the rate of anticipatory licking for the stimulus in individual animals significantly increased. If fosGFP neurons are involved in a learning "engram," we hypothesized that their fluorescence might be increased at the point of learning, so that more cells would be included in the "up" group compared to previous days. Instead, we observed a modest tendency for fosGFP expression to be reduced when we compared fluorescence intensity for individual cells across this restricted time window. Because one animal learned on the first training day (SAT1), we could not compare the percent of increased fosGFP cells compared to the previous day (SAT0). Four out of six animals showed fewer cells in the "up" group than on the prior day, although two out of six animals showed the reverse trend (Fig. 5C).

The degree of change was uncorrelated with the behavior of individual animals, as the performance was not related to the magnitude of fosGFP dynamics (Fig. 5D). There was no significant shift in the cumulative distribution of absolute fluorescence intensity for labeled cells before and after the learning day (Fig. 5E), and tracking expression levels for individual cells organized by intensity rank showed similar results as controls

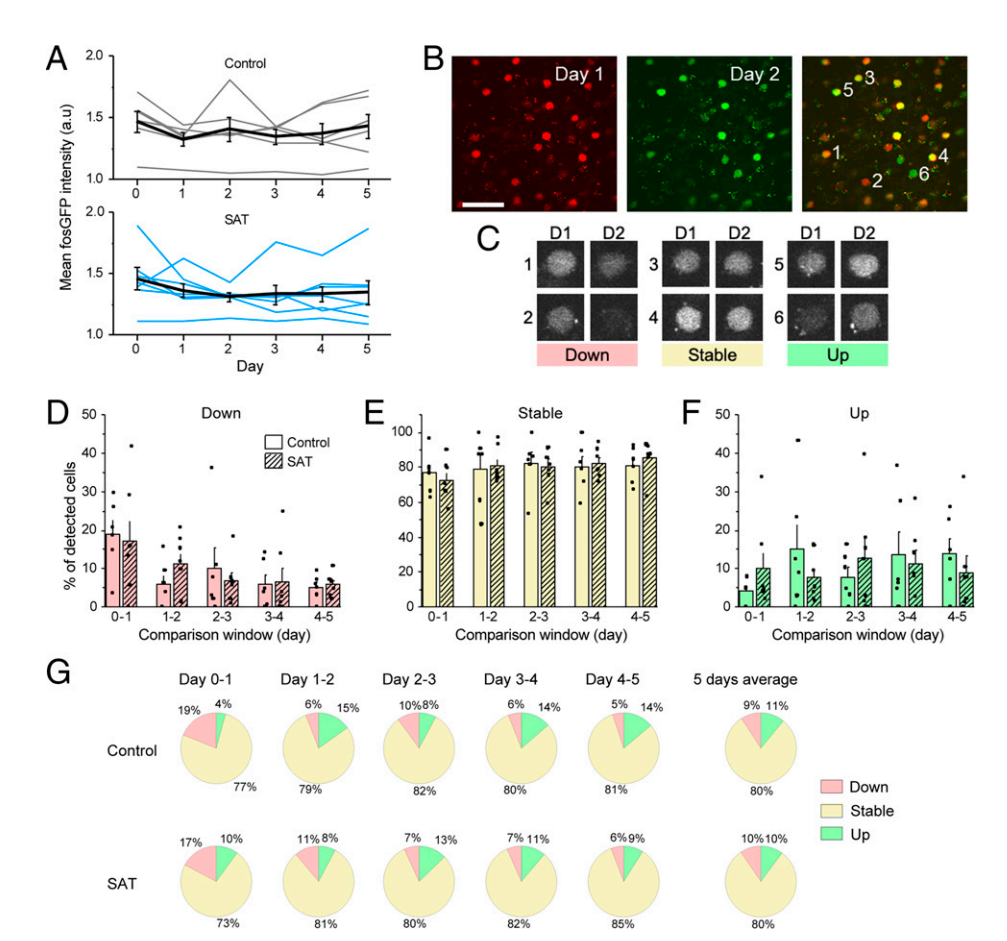


Fig. 4. SAT does not alter the dynamics of fosGFP expression within individual cells. (A) (Top) Mean fosGFP intensity across all detected cells across 5 d of control. Gray lines indicate individual mice. Black line, mean  $\pm$  SEM across six mice. (Bottom) Same as Top for SAT. n=7 mice. (B) Example images of fosGFP-expressing cells in barrel cortex L2/3 across 2 d in a normal home cage. Day 1, red pseudocolor; day 2, green pseudocolor. Cells expressing similar levels of fosGFP on both days show yellow pseudocolor in overlay. (Scale bar, 50  $\mu$ m.) (C) Example down, stable, and up cells from the overlay image in B. Cells were defined as down, stable, or up based on the relative intensity of fosGFP compared to the previous day. (D) Fraction (mean  $\pm$  SEM) of "down" cells out of all detected cells in each 24-h window. n=6 (control), 7 (SAT) mice. Two-sample t test between control and SAT, all nonsignificant. (E) Same as in D for "up" cells. (E) Same as in D for "up" cells.

across the same time window, during which the top 20% of bright cells typically reduced their expression and lower-ranked cells showed a modest increase (Fig. 5F compared to Fig. 3C). These data suggest that in contrast to results from other cortical areas (29–31, 33–35), expression of the IEG c-fos in mouse barrel cortex does not label a cell ensemble selectively engaged during learning.

POm Input to fosGFP Neurons Is Not Increased by SAT. Previously, we have shown that sensory training in an association task leads to an increase in the amplitude of the POm-evoked excitatory postsynaptic current (EPSC), in a broadly sampled population of L2/3 pyramidal (Pyr) neurons from wild-type mice (12). To determine whether fosGFP neurons might be a selective target for this response potentiation, we compared channelrhodopsin (ChR2) POm-evoked EPSCs between fosGFP+ and fosGFP- neurons in L2/3 under basal conditions and after 24 h of SAT. Acute brain slices were prepared from animals and neighboring fosGFP+/-Pyr neurons in L2/3 of barrel cortex were targeted for paired, whole-cell voltage-clamp recordings (Fig. 6 A and B). Consistent with prior studies (18), we found that fosGFP+ neurons showed a small but significantly larger POm-evoked response compared to fosGFP- neurons in slices prepared from untrained mice (1.5fold difference; fosGFP+  $26.63 \pm 6.12$  pA versus fosGFP- 17.85  $\pm$  4.22 pA; n = 4 animals, n = 8 pairs, P = 0.04; Fig. 6 C and E).

We compared the POm-evoked EPSC in fosGFP<sup>+/-</sup> neuron pairs after 24 h of training. Surprisingly, SAT was associated with an increase in the relative amplitude of the POm-evoked EPSC for fosGFP- neurons (0.68-fold difference; fosGFP+ 23.42  $\pm$  6.40 pA versus fosGFP- 34.32  $\pm$  9.72 pA; n=5 animals, n=12 pairs, P=0.25; Fig. 6 D and F). Although variation in the level of ChR2-expression in the POm makes it hard to compare absolute EPSC values across conditions, these data indicate that fosGFP+ neurons are not selectively potentiated by SAT. Indeed, our data suggest that POm inputs to fosGFP-neurons may be selectively enhanced. Thus, although fosGFP+neurons show increased spontaneous- and POm-evoked suband suprathreshold activity under basal conditions (16, 18), they do not appear to compete for stronger POm input potentiation at the early stages of circuit reorganization during SAT.

## FosGFP Expression Can Be Induced by Environmental Enrichment. Because we were surprised to find that SAT in a whisker-dependent task did not detectably alter fosGFP ensembles in S1, we sought to verify that other forms of sensory experience might increase expression of the fosGFP reporter transgene. Previous studies have shown that single-whisker experience (removal of all but one whisker) drives expression of fosGFP in the spared whisker barrel (43, 44), similar to what has been observed using immunohistochemical studies (45), although

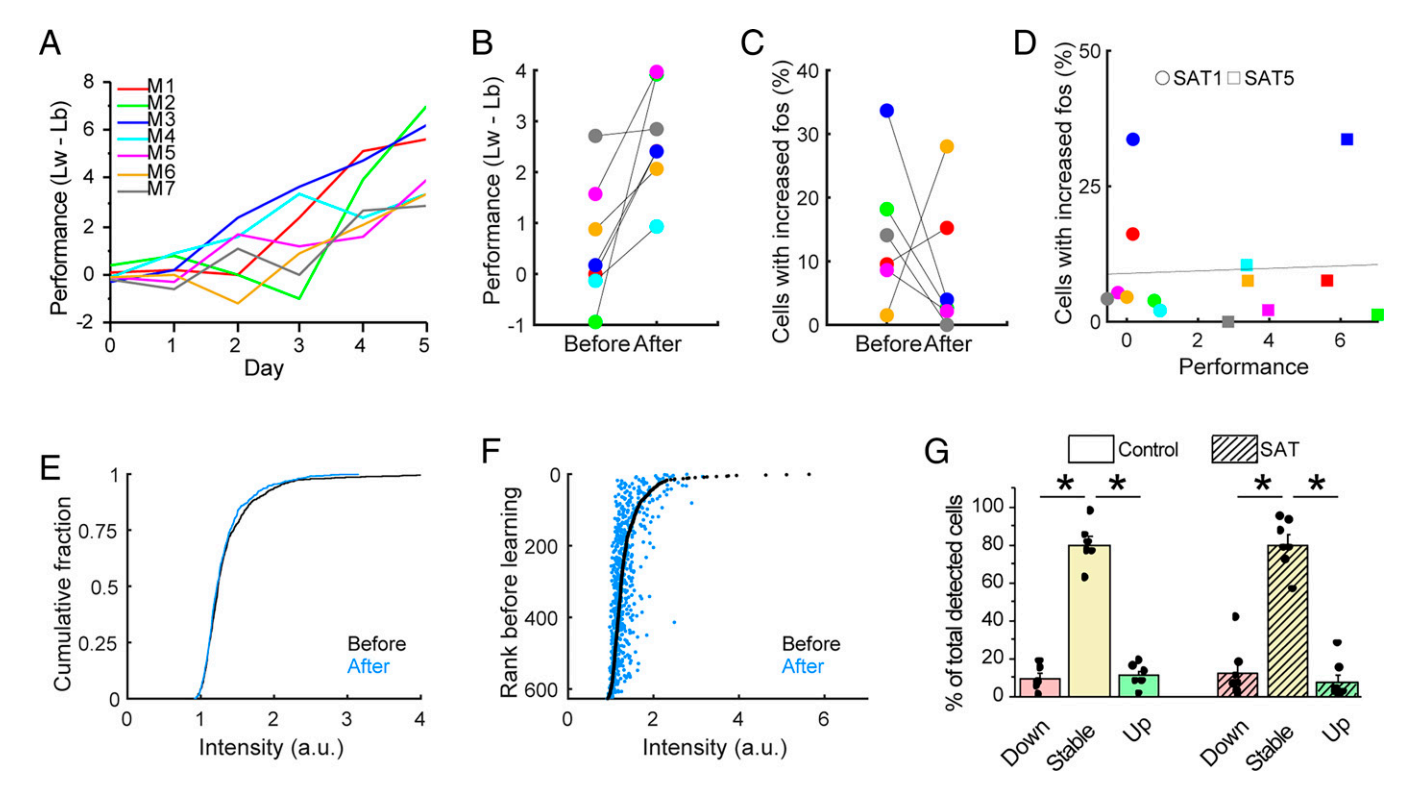


Fig. 5. Learning is not related to increase in fosGFP expression. (A) Behavioral performance is defined as difference between anticipatory lick frequency of stimulus trial ( $L_w$ ) and blank trial ( $L_b$ ). Performance values for each day for each trained animal are shown (n=7). (B) Behavioral performance of the day before learning and after learning. n=7 mice. Same color codes are used for individual animals as in A. (C) Percent of cells with increased fosGFP expression (more than 20% increase) of the day before learning and after learning. n=6 mice. One animal (M4), which learned on the first training day (SAT1), was excluded because there was no previous day to compare. (D) Relationship between behavioral performance and percent of cells with increased fosGFP expression (more than 20% increase). Circles, training day 1 (SAT1). Squares, training day 5 (SAT5). Line indicates a fitting curve with R=0.0540. (E) Comparison of the distribution of fosGFP intensities on the day before learning and after learning. Wilcoxon rank–sum test, P=0.1703. n=627 cells from seven mice. (F) Cells were ranked according to fosGFP intensity on the day before learning. FosGFP intensity of each cell before learning (black) and after learning (blue) was plotted against the rank order before learning. (G) Fractions (mean  $\pm$  SEM) of down, stable, and up cells out of all detected cells during a 24-h window for control group (averaged across 5 d) and during the 24-h window when behavioral performance significantly increased for SAT group. Two-way ANOVA with post hoc Tukey test. n=6 (control), 7 (SAT) mice. \*P<0.05.

this sensory deprivation assay does not reveal stimulus- or behavior-initiated neural ensembles.

To determine whether naturalistic experience with intact whiskers can increase fosGFP expression, we exposed mice to environmental enrichment in the home cage, a potent driver of fos immunoreactivity in rodent barrel cortex (41, 45-47). Mice implanted with a cranial window were housed in a normal cage environment and imaged to characterize baseline expression levels of fosGFP. A variety of tactile enrichment objects were then added to the cage, and mice were imaged after their introduction and exploration of the enriched environment (Fig. 7 A and B). Similar to previous results, FosGFP expression was significantly increased after 6 h of exposure to this enriched environment (Fig. 7C). Cells that increased fosGFP fluorescence signal were distributed across the range of detected cells and were not restricted to increases in the brightest population that had been detected under basal conditions (Fig. 7D). Accordingly, the fraction of cells that increased expression after environmental enrichment ("up" cells) was elevated and the fraction that decreased expression ("down") was suppressed compared to control conditions (Fig. 7E).

We asked whether this increase due to environmental enrichment might also be visible at later imaging time points such as the ones used to monitor ensemble changes during learning. Thus, we tracked fosGFP fluorescence after 1 to 3 d of housing in the enriched environment (*SI Appendix*, Fig. S2). Consistent with the longer half-life of the fosGFP transgene (40) as well as

continuous stimulation from ongoing exposure to the enrichment stimulus (46), the number and intensity of fosGFP neurons remained elevated at later time points.

We conclude that environmental enrichment is sufficient to increase the level of fos expression in the fosGFP transgenic mouse. Thus, absence of a labeled ensemble induced during learning of a sensory association task cannot be attributed to a lack of transgene responsiveness to sensory and behavioral input in the fosGFP transgenic mouse.

## Discussion

Here, we examined how sensory association learning regulates expression of the IEG c-fos in L2/3 of primary somatosensory cortex in a fosGFP transgenic mouse. The training paradigm was optimized to the receptive field properties of fosGFP neurons, using a multiwhisker stimulus coupled with a reward to drive association learning. Despite documented changes in synaptic properties for L2/3 Pyr neurons in this experimental paradigm (12, 48), our results show that fosGFP expression is not enhanced by SAT. Neither training onset nor learning were associated with a marked increase in fosGFP expression either across the population or within individual neurons, although expression could be increased by exposure to an enriched environment. In general, we observed that labeled neurons persisted across time, even in control animals, suggesting that expression is maintained by some ongoing activity in S1 unrelated to the training paradigm. Thus, fosGFP expression in

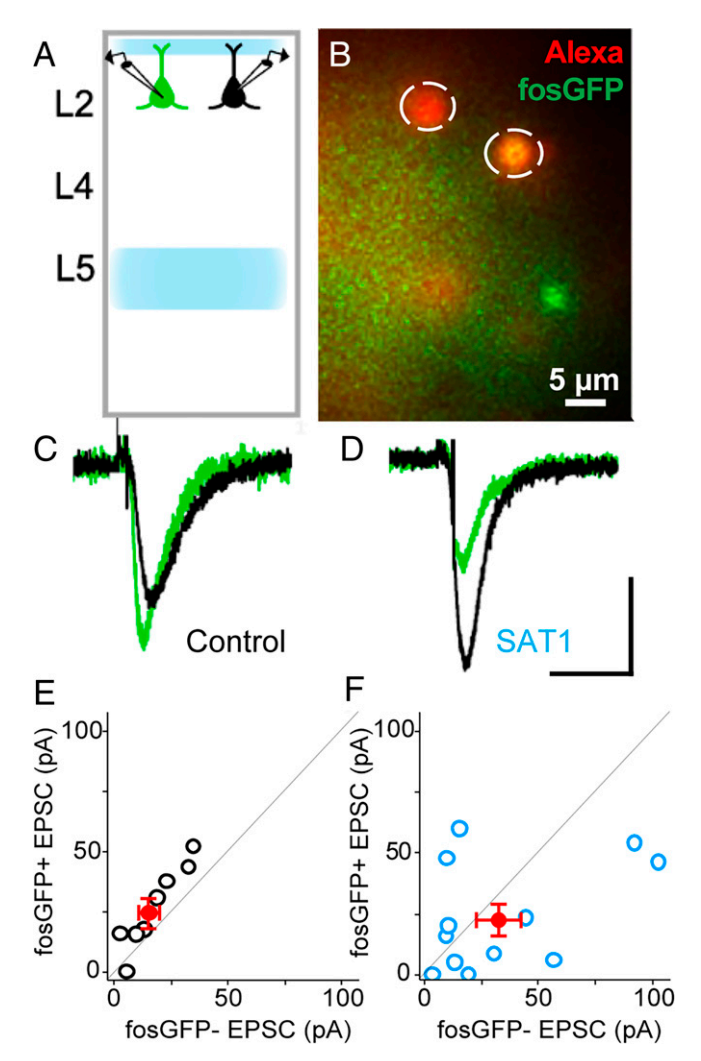


**Fig. 6.** Thalamocortical synaptic potentiation is not concentrated in fosGFP+ cells after SAT. (A) Schematic of in vitro electrophysiology. Blue shades show expression of ChR2 in POm axons innervating the barrel cortex. Dual whole-cell patch-clamp recording was performed in fosGFP- (green) and in fosGFP- (black) cells in layer 2 of the barrel cortex. (B) An example image of dual whole-cell patch-clamp recordings. Alexa 568 cell fill was used to confirm the fosGFP expression of targeted cells. (C) Example average traces of fosGFP+ (green) and fosGFP- (black) cells for control. (D) Same as in C for training day 1 (SAT1). (Scale bar: vertical, 20 pA; horizontal, 50 ms.) (E) Red dot, mean  $\pm$  SEM. POm-evoked EPSC (pA) of fosGFP+ and fosGFP- cells in control (n=4, n=8 pairs). Black dots, individual cell pairs. Two-sample Wilcoxon signed-rank text, P=0.04. (F) Same as in E but for training day 1 (SAT1) animals (n=5, n=12 pairs). Two-sample Wilcoxon signed-rank text, P=0.25.

superficial layers of primary sensory cortex may be an indicator of other network function, not stimulus-specific ensembles that are modified by learning. This contrasts to c-fos expression in other brain areas such as the hippocampus, amygdala, or prefrontal cortex, where training increases c-fos expression and subsequent optogenetic activation of fos-tagged neurons can drive learned behaviors (1, 22–24, 26, 34, 35).

Sensory Cortex and IEG Expression. IEGs have been used to map neural activity across complex neural circuits since their discovery more than 30 y ago. In sensory cortex, IEGs are responsive to sensory stimulation (36), environmental enrichment (41), and sensory deprivation (40), suggesting that they are highly sensitive to alterations in network activity. In vitro studies have

revealed that c-fos expression can be induced both by excitatory synaptic input as well as firing activity (49, 50), although it has been difficult to infer post hoc the precise stimulus that initiated c-fos expression for any given neuron.

IEG expression may not simply reflect recent sensory input. Under basal, home cage condition fosGFP+ neurons show higher spontaneous and whisker-evoked firing activity than neighboring fosGFP- neurons in S1 both in vitro and in vivo, although their intrinsic excitability is not enhanced. Consistent with this, fos-expressing neurons in primary sensory cortex show stronger synaptic excitation, higher network connectivity, and greater spontaneous activity than neighboring unlabeled cells (16, 17, 19). The fact that this activity is preserved in acute brain slices suggests that the factors regulating fosGFP expression might also be local, preserved within the cortical column, and do not require external sensory input to be revealed.

Surprisingly, we did not find that SAT, using a multiwhisker stimulus that was tuned to the response properties of L2/3 fosGFP neurons in mouse barrel cortex, drove an increase in fosGFP expression, activating new neurons, or increasing expression in existing fosGFP+ cells. Although prior studies indicate that fosGFP+ neurons show higher spontaneous and evoked activity, we note that in these studies firing rates for both fosGFP+ and fosGFP- neurons were very low and the difference in firing activity was only approximately twofold (16, 18). It is possible that the previously characterized spontaneous or whisker-evoked firing may be too low (16, 18, 51) to drive fos expression in S1 L2/3 and to alter it during SAT. Indeed, longitudinal imaging revealed that fosGFP+ neurons in superficial layers of S1 were remarkably constant across days, with more than three-quarters of neurons showing fluorescence signal that did not change by >20% each day. Because these dynamics were similar between control and trained mice, we propose that the stimulus required for this sustained expression is maintained over time, possibly through internal dynamics in local networks.

Alternatively, the lack of robust fosGFP induction may be due to the structure of training, which was based on a passive sensory detection task, or the fact that the training was not concentrated in a short time interval to elevate fos expression, as animals carried out several hundred trials stretched out over a 24-h window. However, animals continued to train even in the 4-h time interval immediately preceding the imaging session (mean trial number  $28 \pm 6$  trials; n = 7 mice for 35 total imaging sessions), and the kinetics of fosGFP activation and decay (~2 and 6 h, respectively) (40) are long enough that it was reasonable to expect some cell activation immediately prior to imaging. The constant barrage of sensory input during normal behavior may predominate as the stimulus that maintains fosGFP expression in L2/3 neurons. Indeed, stimulus-specific arcGFP ensembles in V1 could only be revealed against a backdrop of visual deprivation (36). Taken together, we conclude that this SAT paradigm using a multiwhisker stimulus is not sufficient to reveal a task-related ensemble of L2/3 neurons labeled by fosGFP expression.

Capture of Thalamocortical POm Input Potentiation. Our previous studies in wild-type animals indicated that SAT drives increased POm input strength broadly across the population of L2 Pyr neurons (12). We predicted that fosGFP+ neurons would be more likely to show input potentiation, as they show larger excitatory postsynaptic potentials and increased firing with multiwhisker stimulation than fosGFP- neurons (18), and the convergence of presynaptic input followed by postsynaptic spiking known as spike timing-dependent plasticity (STDP) has been proposed as a mechanism by which synaptic strength can be enhanced in vivo (20, 52). In addition, because feature-specific ensembles can be potentiated during reward learning in other

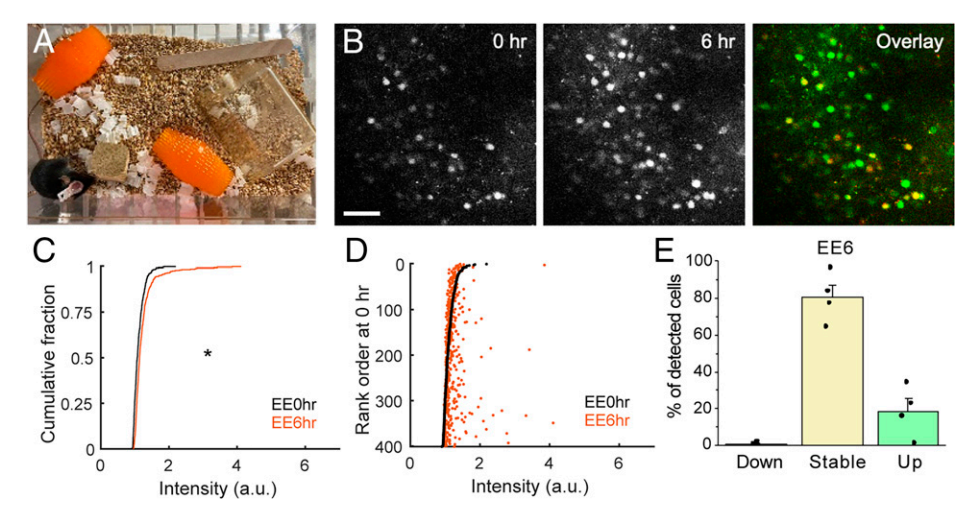


Fig. 7. Enriched environment enhances fosGFP expression. (A) Enrichment items placed in a standard cage. (B) Example images of fosGFP-expressing cells in the barrel cortex L2/3 before enrichment (0 h) and 6 h after enrichment. In overlay, red channel, 0 h, green channel, 6 h. (Scale bar, 50  $\mu$ m.) (C) Comparison of the distribution of fosGFP intensities before enrichment (EE0hr) and 6 h after enrichment (EE6hr). Wilcoxon rank–sum test,  $P = 1.4261 \times 10^{-13}$ . n = 401 cells from four mice. (D) Cells were ranked according to fosGFP intensity before enrichment (EE0hr). FosGFP intensity of each cell at EE0hr (black) and EE6hr (orange) was plotted against the rank order at EE0hr. (E) Fractions (mean  $\pm$  SEM) of down, stable, and up cells during the 6-h window of enrichment. n = 4 mice.

sensory systems (5, 7), we predicted that multiwhisker training might enhance fosGFP expression and that POm inputs to L2/3 fosGFP+ Pyr might be selectively strengthened. Instead, we observed that POm input potentiation seemed to occur in fosGFP— neurons, suggesting a negative correlation between fosGFP expression and thalamocortical synaptic strengthening. The absence of input-specific plasticity for fosGFP+ L2/3 pyramidal neurons suggests that their activity during SAT does not meet the requirements for STDP. Alternatively, synaptic input to fosGFP+ neurons may not be in a state that is permissive for further potentiation during sensory training.

Our results also indicate that increases in POm input strength onto cortical Pyr neurons during SAT (12) are not sufficient to enhance fosGFP expression in L2/3, either in neurons that were fosGFP+ at the onset of training or in fosGFP- neurons. Other studies have suggested that association learning in a whisker-dependent fear conditioning assay reduces overall firing but increases the fidelity and amplitude of stimulus-evoked responses in a subset of L2/3 Pyr neurons (53). It is possible that this was also the case in the present study but that the subset of high-fidelity cells was too small to be identified under our imaging and analysis conditions.

Primary Sensory Cortex Is Different from Other Cortical Areas. Our findings contrast with studies in other brain areas where c-fos induction monitored using the fosGFP transgene or similar reporter constructs has aided the identification of a selective neural ensemble that can report and drive learned behaviors, such as in the hippocampus (22-24), the amygdala (26), hypothalamus (28), and prefrontal and retrosplenial cortex (29, 30, 33-35). These brain areas are notable in that they are more distant from the external world, as they do not receive direct input from sensory thalamus and have more abstract receptive field properties. It is possible that fosGFP expression in primary sensory cortex is related to feedforward sensory input, feedback from higher-order areas, and internal cortical dynamics and that nonsensory components may be critical in S1. Nonetheless, our data are inconsistent with the expectation that reactivation of fos-expressing neurons after SAT in this task will drive a specific sensory percept.

These findings do not invalidate previous studies implicating c-fos in association learning, as has been suggested by some studies in auditory cortex (54). Our analysis was limited to the detection and analysis of the fosGFP transgene, and it is possible that lower levels of c-fos protein are required to initiate the cellular and synaptic plasticity that accompanies circuit reorganization during learning. However, it is useful to note that other transgenic reporters of c-fos expression use essentially the same regulatory and coding regions of the c-fos gene, and the limitations of this transgenic approach may be applicable in other studies (35, 55).

Because imaging was focused on L2/3, it is also possible that fosGFP expression in other cortical layers that were not monitored in this study contain "engram" information. Nevertheless, we note that L2/3 is the site of many experience-dependent changes in synaptic strength and response properties (4–7, 9–12, 53, 56, 57). It is also possible that the engram for learning could be located in areas other than S1, a question that this imaging study did not address. Future studies that monitor IEG expression across the cortical column or other brain areas will be useful to investigate this possibility.

Conclusion. Longitudinal imaging in fosGFP transgenic mice enabled us to directly monitor subsets of fluorescently labeled neurons across time, providing a sensitive assay to detect changes in expression during sensory learning. Our findings suggest that fosGFP expression in superficial layers of barrel cortex is neither a predictive marker for a population of neurons that will be consolidated into a memory "engram" nor a marker for "engram" neurons that sharpen and enhance their response properties with training. Under basal conditions, fosGFP+ neurons were largely preserved across days, much longer than the 3-h half-life of fosGFP expression previously described (40). The stability of the fosGFP neural network in S1 L2/3 suggests that ambient sensory input or internal cortical dynamics may be sufficient to sustain fosGFP expression. Overall, we find that fosGFP expression in superficial layers of primary somatosensory cortex may not provide a useful indicator for stimulus-specific ensembles that are modified by learning.

## **Materials and Methods**

**Animals.** For fosGFP imaging, we used a transgenic mouse line that expresses EGFP under c-fos promoter (Jackson #014135). Adult (>7 wk old) mice were used for cranial window surgery and two-photon in vivo imaging. All mice

loaded at Rutgers University Libraries on January 14, 2022

were single housed for daily imaging. For recording POm-evoked EPSCs in fosGFP+ and fosGFP— pairs, either fosGFP mice or fosGFP mice crossed to Gpr26-Cre mice (Mutant Mouse Resource and Research Center 033032-UCD) were used for better targeting of ChR2 expression in POm. All experimental procedures were conducted in accordance with the NIH guidelines and approved by the Institutional Animal Care and Use Committee at Carnegie Mellon University.

Cranial Window Surgery. Surgery was done under isoflurane anesthesia (4% for induction, 1 to 2% for maintenance). The mouse was put on a heat pad with a temperature control system (FHC 40-90-8D) to maintain body temperature. Dexamethasone (2 mg/kg) was injected subcutaneously right before surgery to reduce brain swelling and/or inflammation. The eyes were covered with Puralube Vet Ointment to protect from drying. Hair on the head was removed with Nair, and skin was cleaned with povidone, then cut out to expose the skull. The skull was scraped with a dental blade (Salvin 6900) to remove periosteum and to roughen the surface for better attachment of glue. On the left hemisphere, S1 barrel field coordinates (3.5 mm lateral, 1 mm posterior to bregma) and a 3-mm-diameter circle centered at the coordinates were marked with a pen. A thin layer of cyanoacrylate glue (Krazyglue) was applied on the skull, then a custom-made head bracket was attached onto the right hemisphere with cyanoacrylate glue and dental cement (Lang Dental, 1223PNK). With a dental drill (Dentsply, 780044), skull was thinned along the 3-mm-diameter circle. Skull was thinned until it showed cracks and became loose. Loose skull was removed by lifting a spot of the thinned region with forceps. Any small bleeding was stopped with saline-soaked gelfoam (Pfizer, 00009032301). Then, a glass window composed of a 3-mm-diameter glass (Warner Instruments, 64-0726) attached to a 4-mm-diameter glass (Warner Instruments, 64-0724) by ultraviolet adhesive (Norland, 717106) was put onto the craniotomy. The window was sealed with 3M Vetbond and then Krazyglue. All exposed skull area except the window was covered with dental cement. A well surrounding the window was built with dental cement for sustaining water for the objective lens. At the end of the surgery, ketoprofen (3 mg/kg) was injected subcutaneously, and the mouse was allowed to recover in a heated cage. Mouse was given at least 3 d of rest before imaging.

Multiwhisker-Dependent SAT. Mice were trained in an automated training home cage (21). Briefly, mice were single housed in a custom-made home cage connected to a freely accessible chamber with a water port and an air puff delivery nozzle. Control fosGFP animals were housed in the training cage where water was delivered without any coupled sensory stimulus. Two out of six animals in the control group showed some significant difference in anticipatory licking at the end of the training period; it is possible that they used the solenoid click as the indicator of water delivery. Because these animals were not trained with the whisker stimulus, they were kept in the control dataset. Training group animals were housed in the training cage for 1 d prior to the onset of training in order to acclimate to the cage and the water delivery system, where water ( $\sim 10~\mu L$ ) was delivered on 80% of nose poke-initiated trials. The remaining trials consisted of a solenoid click but no water delivery (blank trial). During SAT, a gentle air puff (6 psi, 500 ms duration) was delivered to the right facial whiskers, followed by water delivery 1 second later (stimulus trial). For the remaining 20% of trials, there was no air puff and no water delivery (blank trial); this experimental design enabled us to compare anticipatory lick frequency between stimulus and blank trials within the same subject. For fosGFP imaging, we used separate groups for control and SAT; each group went through control condition or training condition for 5 d. For each animal, trial numbers (stimulus + blank trials) and anticipatory lick frequencies (licks occurring in a 300-ms window right before water delivery) were calculated for every 4-h bin using custom MATLAB (The MathWorks) codes.

Acquisition of the stimulus-association was determined by comparing anticipatory lick frequencies for stimulus (Lick<sub>water</sub>; L<sub>w</sub>) versus blank (Lick<sub>blank</sub>; L<sub>b</sub>) trials (12, 21). Mice showed evidence of learning after 1 to 5 d of training, the timing of which varied across individual animals. Learning day was defined as the day when anticipatory lick frequencies of stimulus trials were significantly higher than those of blank trials for the last 20% of the trials of that day [Wilcoxon rank–sum test (12, 21)]. For individual animals, the "day of learning" was typically that day at which *P* reached <0.05 for  $L_w$ - $L_b$ . However, for two animals in the cohort, the *P* value on the last training day did not reach 0.05 (*P* value for  $L_w$  versus  $L_b$  for the last 20% of trials on SAT5 was 0.06 and 0.07). For those animals, we defined the learning day as the fifth day of training (SAT5), when they showed a consistent separation of  $L_w$  and  $L_b$  frequencies. Although this threshold may be subjective, there is a well-recognized variability in animal behavior particularly manifested during early learning (4, 39, 42, 58), an observation that suggests any rigid criterion will

leave a subset of animals as outliers. Importantly, our analysis about fosGFP expression was not affected by excluding these animals from the dataset.

Lick frequencies were compared ( $L_w$ - $L_b$ ) to generate a performance score for 4-h time bins for individual animals. Performance values for each bin were weighted to take into account the number of trials within a given 4-h interval, and values were summed over a 24-h interval to generate a value corresponding to mean behavior performance for that day.

A total of six animals (two males, four females) were used for control, and a total of seven animals (one male, six females) were used for SAT experiments.

**Environmental Enrichment.** Mice were singly housed for 48 h in a standard environment cage (cage only with bedding and small plastic shelter, standard for our animal facility). For enrichment, diverse items (textured plastic objects, wooden block, wooden stick) were placed in the same cage, starting at noon of a given day. Enrichment items were not replaced or removed while the animals were in the enriched caging environment. Animals were removed from the cage and imaged immediately at these timepoints: 1) before enrichment items were placed in the cage (0 h) and 2) at 6, 24, 48, and 72 h after the addition of items. A total of four animals (two males, two females) were used for this experiment.

**Two-Photon In Vivo Imaging.** Imaging was done at the same time of day (noon) every day, under isoflurane anesthesia (4% for induction, 1.5% for maintenance). Imaging sessions finished within  $\sim$ 30 min so that fosGFP expression due to handling was minimized. Because of the delayed time course for fosGFP fluorescence (40), it was unlikely that detected cells were from handling immediately prior to imaging. Mice were put on a heat pad with a temperature control system (FHC 40–90-8D) to maintain body temperature. Blood vessel morphology in 4x (Olympus UPLFLN 4x numerical aperature [NA] 0.13) brightfield was used to find the same imaging spot as the previous session. Pial surface (z=0) was defined as the plane right below the dura matter, which looks like a textured membrane in  $40\times$  (Olympus LUMPLFLN  $40\times$ W NA 0.8) brightfield. In  $40\times$  two-photon mode, X, Y, and Z positions of the neurons were aligned to match the previous session image. A 950-nm excitation (Mai Tai; Spectra-Physics) was used to image fosGFP signals, and emission fluorescence was detected with green photomultiplier tube (PMT).

For each session, we acquired a z stack (100  $\mu m$  to 200  $\mu m$  below pia, step size 2  $\mu m$ ) with a plane size of 300  $\mu m \times$  300  $\mu m$  and resolution of 700 pixel  $\times$  700 pixel, line scan averaged 10 times. Laser power and PMT voltage were kept constant within an animal across imaging sessions. After all imaging sessions were done, the imaging site (which can be identified by the morphology of blood vessels) was marked by either lesion using dental drill or poking the site with a glass micropipette containing methylene blue dye. Then, the brain was fixed and sectioned to confirm that the imaging site was in the barrel subfield.

Image Analysis. Images were acquired with MES software version 6.1.4306 (Femtonics). Raw intensity matrix for each plane image in a z stack was exported from MES and converted to grayscale image by custom MATLAB codes. The intensity value of each pixel ranged from 0 to 65,536 (16-bit image). In a z stack, three representative planes—one each from upper, middle, and lower L2/3 (each portion comprising one-third of the 100-µm-thick z stack in L2/3)—were selected for analysis. Approximately 20 to 50 fosGFP neurons could be identified within an individual imaging field. Identical planes were found for all imaging sessions, and they were precisely aligned with the ImageJ Big Warp plugin. Aligned images were then combined into a single multichannel image for quantification (ImageJ), with each channel corresponding to a different imaging session. In the combined multichannel image, fosGFP cell bodies (regions of interest) were manually marked with circles (diameter 25 pixels), and the average pixel intensity of each region of interest (ROI) for each imaging session was acquired (ImageJ). As long as a cell was detectable in any one of the imaging sessions, that cell's intensity value was obtained for all other imaging sessions no matter how bright or dim it was.

For each cell, changes in the relative intensity of the fosGFP fluorescence signal was defined as  $\,$ 

cell intensity at session N cell intensity at session N-1

Cells for which the day-to-day intensity decreased with a ratio of <0.8 were included in the "down" group. Cells for which the relative intensity was maintained between 0.8 and 1.2 of the previous day's value were included in the "stable" group. Cells for which the day-to-day intensity increased with a ratio >1.2 were included in the "up" group.

Imaging of fosGFP Expression across Cortical Column. A naïve fosGFP mouse that was unexposed to SAT training cage was transcardially perfused with 4% paraformaldehyde, and the brain was removed and fixed with 4% paraformaldehyde for 6 h (short fixation time to reduce degradation of relatively weak fosGFP signals). The brain was sectioned coronally (50  $\mu m$  thickness) and mounted immediately for imaging with confocal microscope (Zeiss 880) in 10x.

Immunostaining of NeuN in fosGFP Brain Sections. Naïve fosGFP mice that were unexposed to SAT training cage were transcardially perfused with 4% paraformaldehyde, and brains were removed and fixed with 4% paraformaldehyde for 6 h (short fixation time to reduce degradation of relatively weak fosGFP signals). Brains were sectioned coronally (50 μm thickness), and slices were washed in phosphate-buffered saline (PBS), then incubated in 10% normal donkey serum in (PBST (0.2% Triton X-100 in PBS) for 1.5 h in room temperature. Slices were incubated in primary antibody solution (NeuN antibody, Cell Signaling 12943, 1:500 in PBST) for 16 to 19 h in 4°C. Then slices were washed in PBST and incubated in secondary antibody solution (goat antirabbit Alexa 594, Thermo Fisher Scientific A-11012) for 2.5 h in room temperature. After washing in PBS, slices were mounted on glass slides and imaged with a two-photon microscope. 950 nm excitation was used to image FosGFP and NeuN (Alexa 594) simultaneously. The imaging field was centered in L2/3 of the harrel cortex

Viral Injection for POm-Evoked EPSC Analysis. ChR2 was introduced into POm in isoflurane-anesthetized fosGFP or fosGFP/Gpr26-Cre mice (postnatal day 15) with stereotaxic injections of AAV1-CAG-hChR2(H134R)-mCherry WPRE.SV40 (Addgene 100054-AAV1, 400 nL), or AAV5-Ef1a-DIO-ChR2-mCherry (UNC Vector core, AV4314J, 500 nL), respectively, in the left POm thalamic nucleus (bregma –1.1, lateral 1.8, depth 3.3 to 3.2 mm) following a small craniotomy using a Hamilton syringe, Stoelting infusing pump, and custom-made injection cannulas. Gpr26-Cre expression is selectively elevated in POm and not ventral posteromedial nucleus of the thalamus (VPM), aiding targeting of this thalamic nucleus. Mice were treated with ketoprofen after injection (5 mg/kg, Sigma-Aldrich). Mice were returned to their home cage and were recovered 8 to 10 d before SAT. The injection site was confirmed by verifying the characteristic pattern of POm axonal terminals in layer 5 (L5) and in layer 1 (L1) of the barrel cortex.

**Slice Preparation.** Mice were anesthetized with isoflurane and decapitated between 12 PM and 2 PM. 350- $\mu$ m-thick barrel slices (one cut, 45° rostro-lateral) (59) were prepared in ice-cold artificial cerebrospinal fluid

- 1. S. A. Josselyn, S. Tonegawa, Memory engrams: Recalling the past and imagining the future. *Science* **367**, eaaw4325 (2020).
- N. Montgomery, M. Wehr, Auditory cortical neurons convey maximal stimulusspecific information at their best frequency. J. Neurosci. 30, 13362–13366 (2010).
- C. M. Niell, M. P. Stryker, Highly selective receptive fields in mouse visual cortex. J. Neurosci. 28, 7520–7536 (2008).
- J. L. Chen et al., Pathway-specific reorganization of projection neurons in somatosensory cortex during learning. Nat. Neurosci. 18, 1101–1108 (2015).
- J. U. Henschke et al., Reward association enhances stimulus-specific representations in primary visual cortex. Curr. Biol. 30, 1866–1880.e5 (2020).
- H. Makino, T. Komiyama, Learning enhances the relative impact of top-down processing in the visual cortex. Nat. Neurosci. 18, 1116–1122 (2015).
- J. Poort et al., Learning enhances sensory and multiple non-sensory representations in primary visual cortex. Neuron 86, 1478–1490 (2015).
- D. E. Feldman, Synaptic mechanisms for plasticity in neocortex. Annu. Rev. Neurosci. 32, 33–55 (2009).
- B. Lendvai, E. A. Stern, B. Chen, K. Svoboda, Experience-dependent plasticity of dendritic spines in the developing rat barrel cortex in vivo. Nature 404, 876–881 (2000).
- S. J. Kuhlman, D. H. O'Connor, K. Fox, K. Svoboda, Structural plasticity within the barrel cortex during initial phases of whisker-dependent learning. J. Neurosci. 34, 6078–6083 (2014).
- Y. J. Sun, J. S. Espinosa, M. S. Hoseini, M. P. Stryker, Experience-dependent structural plasticity at pre- and postsynaptic sites of layer 2/3 cells in developing visual cortex. *Proc. Natl. Acad. Sci. U.S.A.* 116, 21812–21820 (2019).
- N. J. Audette, S. M. Bernhard, A. Ray, L. T. Stewart, A. L. Barth, Rapid plasticity of higher-order thalamocortical inputs during sensory learning. *Neuron* 103, 277–291.e4 (2019).
- S. F. Cooke, M. F. Bear, Visual experience induces long-term potentiation in the primary visual cortex. J. Neurosci. 30, 16304–16313 (2010).
- A. M. LeMessurier, D. E. Feldman, Plasticity of population coding in primary sensory cortex. Curr. Opin. Neurobiol. 53. 50–56 (2018).
- D. J. Margolis, H. Lütcke, F. Helmchen, Microcircuit dynamics of map plasticity in barrel cortex. Curr. Opin. Neurobiol. 24, 76–81 (2014).
- L. Yassin et al., An embedded subnetwork of highly active neurons in the neocortex. Neuron 68, 1043–1050 (2010).

(ACSF) composed of 119 mM NaCl, 2.5 mM KCl, 1 mM NaH $_2$ PO $_4$ , 26.2 mM NaHCO $_3$ , 11 mM glucose, 1.3 mM MgSO $_4$ , and 2.5 mM CaCl $_2$  equilibrated with 95%/5% O $_2$ /CO $_2$ . Slices were incubated for 45 min in the dark before recording.

General Electrophysiology. The same ACSF used for slice preparation was used. Dual whole-cell patch-clamp recordings were performed using an Olympus light microscope (BX51WI) and borosilicate glass electrodes (4 to 8 MΩ) filled with the internal solution composed of 130 mM cesium gluconate, 10 mM Hepes, 0.5 mM ethylene glycol-bis(β-aminoethyl ether)-N,N,N',N'-tetraacetic acid (EGTA), 2.8 mM NaCl, 10 mM tetraethylammonium chloride, 4 mM Mg-ATP and 0.4 mM Na-GTP, and 5 mM QX-314 (lidocaine N-ethyl bromide, Tocris, pH 7.25 to 7.30, 280 to 290 mOsm). Alexa Fluor 568 was added to the internal solution to confirm the morphology of the targeted cells. FosGFP+ and fosGFP- neurons were identified prior to targeting with patch-clamp electrodes. Following the recording, cells were imaged to verify fosGFP expression, their morphology, and their laminar location. Electrophysiological data were acquired using a Multiclamp 700B amplifier (Axon Instruments), digitized with a National Instruments acquisition interface, and collected using MultiClamp and IgorPro 6.0 (Wavemetrics). Data were filtered with 3 kHz and digitized at 10 kHz.

Following whole-cell break-in, a cell was allowed to recover for 3 min. ChR2-expressing POm axons were stimulated by delivering one 5 ms or 10 ms pulse of blue light (470 nm, 3.1 mW light-emitting diode) through a 40x water-immersion objective (Olympus) at the recording site. A targeted cell was voltage-clamped at -70 mV, and POm-evoked EPSCs were collected for 10 trials (0.05 Hz intertrial interval). A pair of fosGFP+ and fosGFP— neurons were targeted for simultaneous recording. Cells were included in the dataset when membrane potential was <-40 mV, and access resistance was <30 M $\Omega$  and was similar between the pair of recorded neurons. The amplitude of the POm-evoked EPSC was averaged across the same and consecutive trials for the recorded pair.

### Data Availability.

All study data are included in the article and/or *SI Appendix*. Raw fluorescence intensity values for each animal subject can be obtained by request from the authors.

ACKNOWLEDGMENTS. The authors thank Joanne Steinmiller for expert animal care; Matthew Mosso for help with histology; members of the A.L.B. laboratory and Y. Kate Hong, Sandra J. Kuhlman, Jean-Sebastien Jouhanneau, and James F.A. Poulet for helpful comments; and Dr. Sunmee Park for contributions to early experiments.

- B. L. Benedetti, Y. Takashima, J. A. Wen, J. Urban-Ciecko, A. L. Barth, Differential wiring of layer 2/3 neurons drives sparse and reliable firing during neocortical development. Cereb. Cortex 23, 2690–2699 (2013).
- J.-S. Jouhanneau et al., Cortical fosGFP expression reveals broad receptive field excitatory neurons targeted by POm. Neuron 84, 1065–1078 (2014).
- M. Xue, B. V. Atallah, M. Scanziani, Equalizing excitation-inhibition ratios across visual cortical neurons. Nature 511, 596–600 (2014).
- G. Q. Bi, M. M. Poo, Synaptic modifications in cultured hippocampal neurons: Dependence on spike timing, synaptic strength, and postsynaptic cell type. *J. Neurosci.* 18, 10464–10472 (1998).
- 21. S. M. Bernhard *et al.*, An automated homecage system for multiwhisker detection and discrimination learning in mice. *PLoS One* **15**, e0232916 (2020).
- X. Liu et al., Optogenetic stimulation of a hippocampal engram activates fear memory recall. Nature 484, 381–385 (2012).
- S. Ramirez et al., Creating a false memory in the hippocampus. Science 341, 387–391 (2013).
- 24. X. Sun et al., Functionally distinct neuronal ensembles within the memory engram. *Cell* 181, 410–423.e17 (2020).
- 25. K. Z. Tanaka *et al.*, The hippocampal engram maps experience but not place. *Science* **361**, 392–397 (2018).
- F. Gore et al., Neural representations of unconditioned stimuli in basolateral amygdala mediate innate and learned responses. Cell 162, 134–145 (2015).
- L. R. Whitaker et al., Associative learning drives the formation of silent synapses in neuronal ensembles of the nucleus accumbens. Biol. Psychiatry 80, 246–256 (2016).
- K. Sakurai et al., Capturing and manipulating activated neuronal ensembles with CANE delineates a hypothalamic social-fear circuit. Neuron 92, 739–753 (2016).
- R. Czajkowski et al., Encoding and storage of spatial information in the retrosplenial cortex. Proc. Natl. Acad. Sci. U.S.A. 111, 8661–8666 (2014).
- M. M. Milczarek, S. D. Vann, F. Sengpiel, Spatial memory engram in the mouse retrosplenial cortex. Curr. Biol. 28, 1975–1980.e6 (2018).
- 31. V. Y. Cao et al., Motor learning consolidates arc-expressing neuronal ensembles in secondary motor cortex. Neuron 86, 1385–1392 (2015).
- J. M. Bossert et al., Ventral medial prefrontal cortex neuronal ensembles mediate context-induced relapse to heroin. Nat. Neurosci. 14, 420–422 (2011).

- L. S. Brebner et al., The emergence of a stable neuronal ensemble from a wider pool
  of activated neurons in the dorsal medial prefrontal cortex during appetitive learning in mice. J. Neurosci. 40, 395–410 (2020).
- T. Kitamura et al., Engrams and circuits crucial for systems consolidation of a memory. Science 356, 73–78 (2017).
- L. Ye et al., Wiring and molecular features of prefrontal ensembles representing distinct experiences. Cell 165, 1776–1788 (2016).
- K. H. Wang et al., In vivo two-photon imaging reveals a role of arc in enhancing orientation specificity in visual cortex. Cell 126, 389–402 (2006).
- H. Xie et al., In vivo imaging of immediate early gene expression reveals layer-specific memory traces in the mammalian brain. Proc. Natl. Acad. Sci. U.S.A. 111, 2788–2793 (2014).
- 38. G. I. Tasaka et al., Genetic tagging of active neurons in auditory cortex reveals maternal plasticity of coding ultrasonic vocalizations. *Nat. Commun.* **9**, 871 (2018).
- S. X. Chen, A. N. Kim, A. J. Peters, T. Komiyama, Subtype-specific plasticity of inhibitory circuits in motor cortex during motor learning. *Nat. Neurosci.* 18, 1109–1115 (2015)
- A. L. Barth, R. C. Gerkin, K. L. Dean, Alteration of neuronal firing properties after in vivo experience in a FosGFP transgenic mouse. J. Neurosci. 24, 6466–6475 (2004).
- J. F. Staiger et al., Excitatory and inhibitory neurons express c-Fos in barrel-related columns after exploration of a novel environment. Neuroscience 109, 687–699 (2002).
- A. Gilad, F. Helmchen, Spatiotemporal refinement of signal flow through association cortex during learning. Nat. Commun. 11, 1744 (2020).
- R. L. Clem, A. Barth, Pathway-specific trafficking of native AMPARs by in vivo experience. Neuron 49, 663–670 (2006).
- R. L. Clem, T. Celikel, A. L. Barth, Ongoing in vivo experience triggers synaptic metaplasticity in the neocortex. Science 319, 101–104 (2008).
- J. F. Staiger et al., Exploration of a novel environment leads to the expression of inducible transcription factors in barrel-related columns. Neuroscience 99, 7–16 (2000).

- S. Bisler et al., Expression of c-Fos, ICER, Krox-24 and JunB in the whisker-to-barrel pathway of rats: Time course of induction upon whisker stimulation by tactile exploration of an enriched environment. J. Chem. Neuroanat. 23, 187–198 (2002).
- R. K. Filipkowski, M. Rydz, B. Berdel, J. Morys, L. Kaczmarek, Tactile experience induces c-fos expression in rat barrel cortex. *Learn. Mem.* 7, 116–122 (2000).
- D. A. Kuljis, E. Park, S. E. Myal, C. Clopath, A. L. Barth, Transient and layer-specific reduction in neocortical PV inhibition during sensory association learning. bioRxiv [Preprint] (2020). https://doi.org/10.1101/2020.04.24.059865 (Accessed 6 December 2021).
- R. D. Fields, F. Eshete, B. Stevens, K. Itoh, Action potential-dependent regulation of gene expression: Temporal specificity in ca<sup>2+</sup>, cAMP-responsive element binding proteins, and mitogen-activated protein kinase signaling. J. Neurosci. 17, 7252–7266 (1997).
- S. M. Luckman, R. E. Dyball, G. Leng, Induction of c-fos expression in hypothalamic magnocellular neurons requires synaptic activation and not simply increased spike activity. J. Neurosci. 14, 4825–4830 (1994).
- S. Crochet, J. F. A. Poulet, Y. Kremer, C. C. H. Petersen, Synaptic mechanisms underlying sparse coding of active touch. *Neuron* 69, 1160–1175 (2011).
- 52. D. E. Feldman, The spike-timing dependence of plasticity. Neuron 75, 556-571 (2012).
- A. Gdalyahu et al., Associative fear learning enhances sparse network coding in primary sensory cortex. Neuron 75, 121–132 (2012).
- L. de Hoz et al., Blocking c-fos expression reveals the role of auditory cortex plasticity in sound frequency discrimination learning. Cereb. Cortex 28, 1645–1655 (2018).
- L. A. DeNardo et al., Temporal evolution of cortical ensembles promoting remote memory retrieval. Nat. Neurosci. 22, 460–469 (2019).
- P. Mégevand et al., Long-term plasticity in mouse sensorimotor circuits after rhythmic whisker stimulation. J. Neurosci. 29, 5326–5335 (2009).
- D. J. Margolis et al., Reorganization of cortical population activity imaged throughout long-term sensory deprivation. Nat. Neurosci. 15, 1539–1546 (2012).
- K. V. Kuchibhotla et al., Parallel processing by cortical inhibition enables contextdependent behavior. Nat. Neurosci. 20, 62–71 (2017).
- G. T. Finnerty, L. S. E. Roberts, B. W. Connors, Sensory experience modifies the shortterm dynamics of neocortical synapses. *Nature* 400, 367–371 (1999).